

To Perceive the Mix of GTA Parameters on the Outside of AISI304 Stainless Steel that Gives Improvement in the Properties AISI304 Tempered Steel in the Changed Layer

Tej Ram Sahu¹ and Ashok Sharma²

^{1,2}Department of Mechanical Engineering

^{1,2}Shri Shankaracharya Institute of Technology & Management, Chhattisgarh, India

Abstract— Quality of modified specimens mainly depends on the mechanical properties of the alloying material and the warmth influenced zone (HAZ), which is in direct connection with the kind of welding procedure and its parameters. Dab width and profundity of entrance were by and large impacted by welding process parameters i.e., welding current, travel speed, remain off separation, protecting gas stream rate, tip edge and voltage and further rmore it assumes a significant job in deciding the surface properties of the changed layer, for example, surface hardness, wear rate and so on. In this investigation, impact of surface properties by fluctuating the procedure parameters has been examined on the AISI 304 tempered steel bars of size 30x30x100 mm surface adjusted with economically unadulterated titanium of thickness 0.3 mm. The surface alloying of AISI 304 hardened steel with Ti were completed by Gas Tungsten Arc (GTA) under N₂ climate. Optical microscopy was utilized to discover the microstructure and Energy Dispersive Spectroscopy (EDS) was utilized to discover the level of substance sythesis in the Ti altered layer. The X-Ray Diffraction examination (XRD) was utilized to describe the Ti adjusted layer. The surface hardness and the wear rate of the Ti changed layer were explored by Vickers hardness testing machine and Pin-on-circle wear testing machine. Results showed that perception of the microstructure of the surface alloyed layer uncovers grain refinement. The intermetallic mixes FeTi, TiN and TiNi were shaped utilizing XRD examination. The hardness expanded from 264 HV for the substrate to 2679 HV for Ti adjusted layer. The Coefficient of contact is practically consistent for substrate and surface alloyed example. The EDAX investigation demonstrates an expansion in the Ti content on the altered layer when contrasted and the piece of the substrate. A set of examinations has been led to gather the trial information utilizing focal composite plan of reaction surface philosophy. In light of the recorded information, the ANOVA tables have been created. Further a model approval has been done to affirm the estimation of yield reactions, for example,

profundity of infiltration, hardness and wear rate that are equivalent to the ideal worth which are determined utilizing ANOVA table.

Keywords— GTA parameters, AISI304 stainless steel, tempered steel.

I. INTRODUCTION

1.1 Background

Stainless steels strength, prevention of corrosion attack and low care makes it the supreme material, but poor surface hardness and high wear rate are the core problems to medical, commercial and industrial sectors. AISI304 stainless steel have been broadly used in aerospace, food processing, nuclear and biomedical because of its high corrosion resistance.

The stainless steel normally has great consumption obstruction, in light of the fact that, in the air, chromium in its structure joins with oxygen of the air to shape a slight latent covering of chrome oxide on the outside of the tempered steel. Be that as it may, for the situation the hardened steel is carried into contact with a destructive liquid, for example, hydrogen sulfide, chloride particle and a high temp water containing oxygen, setting erosion or breaks because of consumption are obligated to happen in the outside of the tempered steel. Run of the mill results of hardened steel that are presented to surface treatment are apparatuses and molds, siphon parts, direction, channels, gears, screws, valves, careful instruments. [1].

Usually, coatings are applied onto the surface of the parent material in order to obtain the preferred properties. For the coating purpose, various traditional methods like electroplating, electroless plating, Physical Vapour Deposition (PVD), Chemical Vapour Deposition (CVD) and thermal spraying were commonly used. However, the coatings obtained by these methods are likely to eradicate under severe loading conditions. In order to overcome such complications, researchers have

adopted a new method called Surface Modification Process (SMP).

1.2 Types of Stainless Steel

Stainless steels are characterized as iron base combinations which contain at any rate 10.5% chromium. The slim however thick chromium oxide film which structures on the outside of a treated steel gives erosion obstruction and counteracts further oxidation. There are five kinds of hardened steels relying upon the other alloying increments present, and they go from fully austenitic to fully ferric. Austenitic tempered steel incorporates the 200 and 300 arrangement of which type 304 is the most well-known. The essential alloying increases are chromium and nickel. Ferritic treated steels are non-hardenable Fe-Cr compounds. Types 405, 409, 430, 422 and 446 are illustrative of this gathering. Martensitic tempered steels are comparative in synthesis to the ferritic gathering however contain higher carbon and lower chromium to allow solidifying by warmth treatment. Types 403, 410, 416 and 420 are illustrative of this gathering. Duplex hardened steels Stainless steels quality, a version of consumption assault and low consideration makes are provided with a microstructure of around equivalent measures of ferrite and austenite. They contain generally 24% chromium and 5% nickel. Their numbering framework is excluded in the 200, 300 or 400 gatherings. Precipitation solidifying tempered steels contain alloying increments, for example, aluminum which enable them to be solidified by an answer and maturing heat treatment. They are additionally ordered into sub bunches as martensitic, semi-austenitic, and austenitic precipitation solidifying tempered steels. They are recognized as the 600-arrangement of tempered steels.

1.3 AISI304 Stainless Steel

Stainless steel types 1.4301 are otherwise called AISI304. AISI304 is the most adaptable and broadly utilized hardened steel.

It is still some of the time alluded to by its old name 18/8 which is gotten from the ostensible creation of AISI304 being 18% chromium and 8% nickel. AISI304 tempered steel has phenomenal consumption obstruction in a wide assortment of situations and when in contact with various destructive media.

AISI304 tempered steel has great protection from oxidation. AISI304 tempered steel can't be solidified by warmth treatment. Table 1.1 demonstrates the ordinary physical properties of AISI304 hardened steel.

AISI304 hardened steel is commonly utilized for assembling of cylinders, distillery gear, pharmaceutical generation hardware, springs, nuts, fasteners, screws and restorative inserts.

1.4 Commercially Pure Titanium (CP-Ti)

Titanium is recognized for its high strength-to-weight ratio. It is a strong metal with low density that is quite ductile, lustrous, and metallic-white in colour. The relatively high melting point makes it useful as a refractory metal. It is paramagnetic and has fairly low electrical and thermal conductivity.

Commercial (99.2% purity) grades of titanium have ultimate tensile strength of about 434 MPa, equal to that of common, low-grade steel alloys, but are less dense. Titanium is 60% denser than aluminium, but more than twice as strong as the most commonly used 6061-T6 aluminium alloy. The titanium used for surface alloying of AISI304 stainless steel was CP-Ti, grade 2, 300µm thick sheet. The typical physical properties of CP-Ti are shown in Table 1.2.

Table 1.2 Typical Physical properties of CP-Ti

S.No	Property	Value
1	Density	4.50 g/cm ³
2	Melting Point	1600-1670°C
3	Modulus of Elasticity	116 GPa
4	Tensile Strength	434 MPa
5	Compression Strength	182 MPa
6	Hardness Vickers (HV)	210

1.5 Surface Modification Process

Surface modification process (SMP) is emerging as a method alternate to the traditional coating processes in order to enhance the tribological and corrosion properties of nonferrous and ferrous alloys.

SMP can be defined as the process of modifying the surface of a material by bringing out changes in the properties different from those found originally on the surface of a material. The principal aim of the application of surface modification technique is to form hard and ultrafine structure on the surface layer so that the properties are improved. SMP can be classified into two categories: namely, i.) Surface Refining Process (SRP) and ii.) Surface Alloying Process (SAP).

1.5.1 Surface Refining Process

In the SRP, as shown in Figure 1.1, the surface of the substrate is melted by using an appropriate heat source to form a molten pool, and subsequently the heat source is moved progressively across the length of the substrate so that a solidified layer forms on the surface of the substrate upon solidification. In the SRP, a fine grain structure forms during solidification as a result of the rapid cooling experienced in this process. As a result of the fine grain structure, the modified layer shows improved properties. In contrast to the traditional coating methods, in the SRP, the modified layer is integral to the substrate. Therefore, it is expected that the components treated by this method can carry a higher load than those coated by the traditional methods. The modified surface will exhibit superior wear resistance. In the method surface alloying, first alloying components or fired particulates are set as coatings, sheets, powder or glue onto the outside of the base metal (substrate). Tailing it, utilizing a picked warmth source, both the component or particulates and the base metal are softened to make a combination zone. The warmth source is at that point, logically moved along the length of the base metal to frame a bound together combination layer on the outside of the base metal upon hardening. Figure 1.2 delineates the surface alloying process with a covering of the alloying component on the outside of the substrate

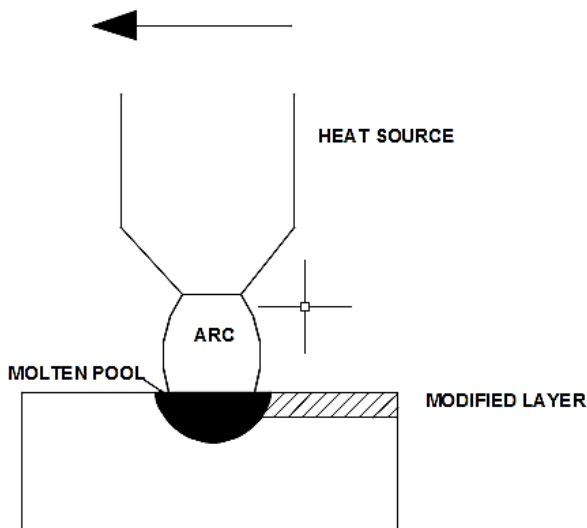


Figure 1.1 Surface Refining Process

1.5.2 Surface Alloying Process

In this procedure, an amalgam not the same as the substrate may shape. Further, there is a plausibility of shaping intermetallic compound in the adjusted layer because of the expansion of different sorts of alloying components onto the surface. Likewise, because of the quick cooling experienced during the hardening stage,

the outside of the base metal (substrate) is refined into fine structure all through the surface. The arrangement of the intermetallic mixes and the refinement of the surface are the primary purposes behind the improved properties of the altered layer. The surface alloying procedure separates itself from the traditional covering systems with the alloyed changed layer staying essential to the base metal. Consequently, scientists visualize that such surface alloyed metals can withstand higher loads in the administration contrasted with those covered by the customary methods. The alloyed surface is additionally expected to have a high wear obstruction. In the literature, three main approaches have been practiced for carrying out the surface alloying process. With the first approach, the conventional coating techniques such as electro-plating or electro-less plating have been employed to coat the base metal with the alloying element. The element fuses onto the surface of the base metal during the progress of the process. Another approach followed for alloying the base metal is to powder the alloying element and mix it with appropriate binders. The formed paste is then laid on the base metal, followed by the melting and fusing with the base metal using a heat source. The last technique includes bolstering the alloying component or clay particulates (powdered structure) into the liquid pool by utilizing a powder feeder contraption.

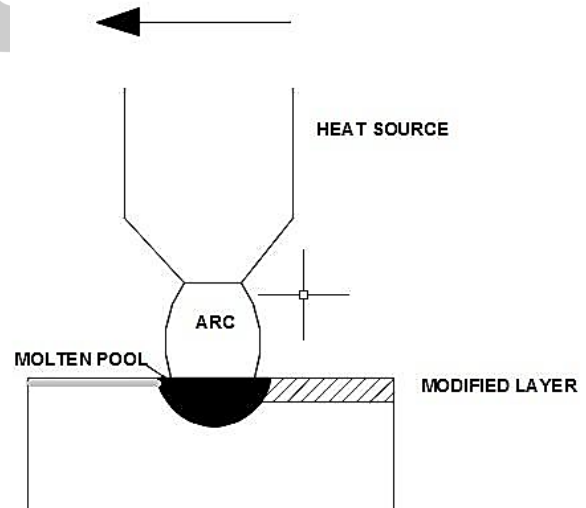


Figure 1.2 Surface Alloying Process

In SAP, a fine grain structure of the changed layer can be accomplished upon hardening because of quick cooling of the liquid layer. The improvement in surface properties is accomplished because of the development of a fine grain structure. Different alloying components like Ni, Cr, Ti, Mo and so forth., can be added to the liquid pool so another composite with wanted properties can be framed upon cementing. Further, because of the fast cooling as well as amalgam

expansion, hard intermetallic mixes may likewise frame in this procedure. Furthermore, very refractive clay particulates like TiC, B4C, SiC and so on., can likewise be added to the liquid pool so as to shape a metal lattice composite. Thus, the altered layer displays a high hardness because of the nearness of the earthenware particles. The altered layer can likewise go about as a warm obstruction in certain occurrences and henceforth it might discover applications where the segment is utilized in a high temperature condition. The geometry of the changed layer and the grouping of the alloying component in the adjusted layer are the basic factors that choose the surface properties like wear opposition, consumption obstruction just as the surface hardness. The liquid pool geometry and the alloying component fixation rely on the covering strategy and the warmth source utilized.

1.6 Types of Heat Source

In the literature, it has been reported that the electron beam and laser beam heat sources have been selected for this application. The Gas Tungsten Arc (GTA) heat source has been considered by a few researchers. In the electron beam, process a power density of 100 kW/cm² is used. Due to the high intensity of the e-beam, it is likely that the alloying element may vaporize. The limitations associated with the e-beam process are the high cost of the equipment, the requirement of a high vacuum environment that restricts the size of the component, low productivity and low efficiency. Further, the depth of the modified layer is very low that limits the service life of the components. Finally, the e-beam process is considered to be not cost effective for the surface alloying process. The process of laser surface melting involves the use of an energy-intensive laser heat source to melt the surface of the base metal. The popular heat source is a continuous wave CO or an Nd:YAG laser beam. The shielding gas preferred is the noble Nitrogen gas. The laser heat source shows a variation in intensity because of the reflectivity of the base metal surface and therefore, it is difficult to achieve a uniform modified layer. The efficiency of the laser is around 16%. Due to the high intensity of the laser beam, it is likely that the alloying element may vaporize.

The width of the modified layer is not high and therefore, it requires a several passes to completely cover a given surface. As a result, the efficiency of the laser pillar procedure is exceptionally low. In perspective on the restrictions of the e-shaft and laser pillar warmth sources, the GTA has been considered as another warmth hotspot for the surface refining/alloying forms. The GTA warmth source is

described with its high warm effectiveness (75%), high efficiency, cheap gear cost and simplicity of activity. Additionally, the width and profundity of the adjusted layer are high when contrasted with those of e-pillar/laser shaft process. Further, the GTA procedure factors can be effectively controlled so the ideal width and profundity of the adjusted layer can be accomplished. At last, enormous segments can be effectively prepared with the GTA warmth source.

1.7 Design of Experiments

A multi-level full factorial design was selected as a statistical design of experiment (DOE) technique to develop the semi-empirical mathematical models correlating the process parameters to each measured responses. Figure 1.3 shows the 3 level CCD matrix model for experimentation. Response surface methodology is a useful design of experiment method that is gaining popularity. This includes a review of basic experimental designs for fitting linear response surface models, in addition to a description of methods for the determination of optimum operating conditions.

The steps of response surface methodology are:

- (i) Developing experimental strategy for selecting independent variables.
- (ii) Statistical modelling to build an approximate relationship between the response and process variables.
- (iii) Optimization for finding values of process variables producing desirable values of the response.

In RSM, an approximate model is needed to develop for the true response surface. The approximated model is constructed utilizing observed data from the process or system. Multiple regression analysis is commonly used for this. Usually, a second-order polynomial equation is used in RSM. The commercial statistical software Design- Expert V10.1.2 was used to create the design matrix and analyze the experimental data.

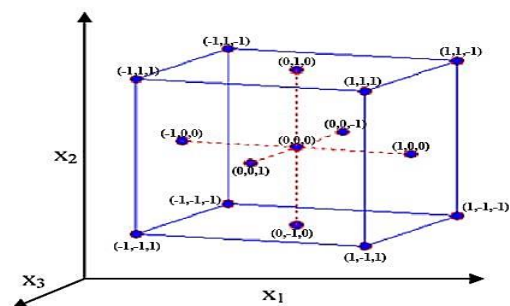


Figure 1.3 3-level CCD Matrix

1.8 Present Work

The greater part of the exploration works referred to in the writing were directed to research the impact of alloying utilizing laser or e-shaft, particle implantation, plasma nitriding and carburizing. Be that as it may, an examination superficially alloying of the AISI304 hardened steel with Ti by utilizing the gas tungsten circular segment as the warmth source has not been accounted for in the writing. Hardened steel is a generally utilized designing compound in fluid taking care of frameworks and pressure driven apparatus due to its great erosion obstruction, great processability, and moderately ease. Since AISI304 treated steel has a low hardness and present examination is attempted to improve the hardness property by the surface alloying process.

1.9 Objective

The objectives of the present research work are as per the following:

1. To perceive the mix of GTA parameters on the outside of AISI304 Stainless steel that gives improvement in the properties in the changed layer.
2. To structure a Ti surface alloyed layer on the outside of the AISI304 tempered steel substrate by utilizing the surface alloying process.
3. To watch the microstructure of AISI304 hardened steel and changes to it because of surface alloying with Ti.
4. To evaluate the impact of Ti expansion to the outside of the AISI304 hardened steel substrate on the hardness of the surface Ti surface alloyed AISI304 treated steel.
5. To evaluate the upsides of utilizing GTA as the warmth hotspot for the surface alteration process when contrasted with the laser/e-bar source.

1.10 Conclusion

This chapter introduces the surface refining process and surface alloying process the relevance of surface alloying AISI304 stainless steel in order to improve the surface properties, namely surface hardness. Additionally, the justification for carrying out the present study, objectives and organization of the thesis are presented.

II. LITERATURE REVIEW

2.1 Literature regarding Design of Experiments (DOE)

F. Vakili- Farahani et al. [2] Laser Beam Welding (LBW) combined with "wobble impact" (quick oscillation of the ray) is exceptionally encouraging for high exactness small scale joining industry. For this procedure, also to the regular LBW, the laser welding process parameters assume an extremely huge part in deciding the nature of a weld joint. Accordingly, four process parameters (laser power, wobble frequency,

number of rotation and focused position) and 5 responses (depth, HAZ, width, hardness, area of HAZ and area of fusion zone) were explored for spot welding of Ti6Al4V alloy using a DOE approach. This paper presents exploratory outcomes demonstrating the impacts of varying the considered most imperative process parameters on the spot weld nature of Ti6Al4V. Semi-empirical technical models were produced to associate laser welding parameters to each of the deliberate weld responses. If the models were then analyzed by different techniques, for example, ANOVA. These models not just permit a superior knowledge of the wobble laser welding process and expect the method accomplishment additionally decides optimum process parameters. Therefore, optimum arrangement of process parameters was resolved considering certain quality criteria set.

Nikhil Kumar et al. [3] In the present work, AISI 304 stainless steel sheets are laser welded in butt joint configuration utilizing a mechanical control 600 W beat Nd:YAG laser framework. The goal of the work is of twofold. The study expects to find out the impact of angle on the weld pool geometry, tensile properties and microstructure of the welded joints. Also, an arrangement of analyses are conducted, as indicated by RSM, to examine the impacts of process parameters, specifically, laser power, incident angle of beam and welding speed on extreme elasticity by building up a second order polynomial equation. Study with three angles of laser beam 83 deg, 89.7 deg and 85.5 deg has been displayed in this work. It is studied that the weld pool geometry has been significantly changed with the deviation in angle. The weld pool shape at the top surface has been modified from semi-round or about circular shape to tear drop shape with decline in angles. Concurrently, fine columnar dendritic, planar and coarse columnar dendritic structures have been detected at 83 deg, 89.7 deg and 85.5 deg. Weld metals with 85.5 deg has higher portion of carbide and d-ferrite precipitation in the austenitic lattice contrasted with other weld conditions. Thus, weld metal of 85.5 deg accomplished higher hardness of 280 HV and tensile of 579.26 MPa taken after by 83 deg and 89.7 deg angle welds. Moreover, the expected max value of UTS of 580.50 MPa has been accomplished for 85.95 deg angle utilizing the equation where other two ideal parameter settings have been acquired as laser energy of 455.52 W with welding speed of 4.95 mm/s. This perception has been agreeably approved by three confirmatory tests.

Benyounis K.Y et al.[4] Laser butt-welding of medium carbon steel was examined utilizing CW 1.5 kW CO₂ laser. The impact of welding speed (30–70 cm/min),

point of convergence position (−2.5 to 0 mm) and laser power (1.2–1.43 kW) on the heat input and the weld-bead geometry (i.e. welded zone width (W), penetration (P) and heat influenced zone width (W_{HAZ})) was researched utilizing RSM. The investigational plan depended on Box–Behnken framework. Linear and quadratic polynomial conditions for calculating the heat input and the weld-bead geometry were created. The outcomes show that the suggested models expect the responses satisfactorily inside the boundaries of welding parameters being utilized. It is recommended that regression equation can be utilized to find ideal welding conditions for the desirable criteria.

Selvamani S.T et al.[5] In this present work, the investigation of process parameters on chemical, mechanical and metallurgical properties of AISI1035 steel bars of 12 mm width joints formed using friction welding is examined. The joints made with different process parameter arrangements are subjected to cyclic potentiodynamic polarization tests, hardness test and tensile test. The properties, for example, notch tensile, tensile and yield strength, % elongation, and Vickers's hardness, flash formation, fully deformed zone (FDZ) and pitting corrosion has been analyzed for high level and low level process parameters. The enhanced procedure variable is acquired by utilizing RSM. The integrity of the welds has been examined using high magnification optical microscopy. The crack surface of the tensile test specimens is analyzed by utilizing Scanning Electron Microscope (SEM) and Energy-dispersive X-beam spectroscopy (EDAX).

Paventhan R et al.[6] Friction Welding (FW) is a process of solid state joining which is utilized widely as of late because of its points of interest, for example, ease of manufacturing, low heat input, environment kindness and production efficiency. FW can be utilized to join various sorts of ferrous and non-ferrous metals that can't be welded by usual fusion welding forms. The process parameters, for example, friction pressure and time, forging force and time assume the genuine parts in deciding the quality of the joints. In this examination an effort was made to build up an empirical relationship to expect the tensile strength of FW AA 6082 aluminum alloy and AISI 304 austenitic SS joints, consolidating above said parameters. RSM was associated to enhancing the FW process parameters to achieve the max tensile strength of the joint.

Paventhan R et al.[7] Friction Welding (FW) is a solid state joining process utilized widely as of now inferable, for example, ease of manufacturing, low heat input, environment friendliness and high production

efficiency. Materials hard to be welded by fusion welding process can be effectively welded by FW. An effort was made to build up an empirical relationship to calculate the tensile strength of FW AISI 1040 grade medium carbon steel and AISI 304 austenitic SS, consolidating the process parameters, for example, friction time and pressure, forging time and pressure, which have improbable impact on quality of the joints. RSM was applied to improve the FW process parameters to achieve max tensile strength of the joint. The max tensile strength of 543 MPa could be acquired for the joints created under the welding circumstance of friction and forging pressure of 90 MPa each and friction and forging time of 6 s each.

Selvamani S.T et al[8]. In this work, 12 mm dia of AISI 1035 grade steel rods are Friction Welding (FW) with a mean to enhance the process parameters. The joints are made with different process parameter mixtures (fusing ANOVA strategies) subjected to tensile test. The empirical relationship is built up to anticipate a UTS, % of elongation and notch strength of the welded joints. The model's consistency has been tested. The tensile properties, microstructures, SEM, EDAX and the hardness of the welded samples have been studied and displayed in this review.

Kumar R et al. [9] A technique to choose close ideal settings of the process parameters in Friction Welding (FW) was projected. The accomplishment of the FW process depends on different input parameters like upset pressure and time, friction time and pressure and output parameters like material loss, hardness and tensile strength. Ti–6Al–4V and SS304L (SS) materials were joined by FW process utilizing interlayer strategies. The Box–Behnken design and RSM were applied to choosing the quantity of investigations to be performed and recognize the ideal process parameters for acquiring better joint quality. The results were profoundly favourable. Join quality of 523 MPa was gotten at a friction and upset pressure of 12 N/mm² and 40 N/mm², upset and friction time of 7 s and 12 s.

2.2 Literature regarding Surface Alloying (SA) process
Mridha S [10] The possibility of building up a hard titanium nitride layer has been considered by liquefying financially unadulterated titanium (CP-Ti) surfaces underneath the TIG burn in an unadulterated N₂ air. The setting of titanium with TIG light of vitality densities stretching out from 46 MJ m^{−2} to 182 MJ m^{−2} conveyed a liquid layer of more than 1 mm thickness. The geographies of the fluid tracks covered at vitality densities more than 68 MJ m^{−2} had

undulating tracks and they are inverse to the covering course. However, the tracks covered at lower vitality densities of 46 MJ m⁻² and 55 MJ m⁻², conveyed cell kind surface structures. Porous edges were accessible in all of the tracks covered in the N₂ climate at different vitality densities. Those tracks covered at higher vitality densities made surface splitting along the track width, and they spread down to the dissolve zone. The resolidified soften microstructures contained non-uniform dissemination of dendrite populaces. The XRD examination at different profundities of the dissolve cross area revealed that the TiN stage controls the liquid pool microstructure. The surface hardness of around 2000 HV have been achieved from the tracks. All tracks are covered at different vitality densities produced hardness profiles with enduring declines in hardness at a higher molten depth. This displays the hardness improvement is uncommonly related to the dendrite populace in the liquid pool, which was found to diminish at depth because of the lower gathering of nitrogen.

Hojjatzadeh S.M.H et al.[11] The effect of contrasting the collection of N₂ to the protecting gas on SA of an AISI 1045 steel as a base metal with a preplaced layer of ferrotitanium (FeTi) powder during GTA were inquired about. The cross-sectional zone and entrance of the alloyed layer extended with the N₂ content in the protecting gas. Diverse N₂ substance in the protecting gas caused the advancement of two key microstructure: (1) Ti (C_xN_y) in a matrix of eutectic structure of ferrite (α), ferrite (α) and Fe₂Ti at a low N₂ substance and (2) TiN dendrites coursed in a ferrite (α)- Fe₃C cross section at a high N₂ content. Model softened under argon climate was consolidated with TiC in a matrix of eutectic structure of ferrite (α), ferrite (α) and Fe₂Ti. The last correspondingly affirmed the expansion in hardness, which could be supported to the presence of the low disintegration of the layer and fine eutectic structure.

SonerBuytoz and Mustafa Ulutan (2006)[12] In this audit, an austenitic SS surface was covered with different silicon carbide powder substance. The procedure parameters were changed with a particular ultimate objective to choose their effect on the covering microstructure. The outcomes affirmed that the silicon carbide particles are completely separated during the age. At the lower powder content, the microstructures involved dendrites. However, M₇C₃ fundamental carbides were created at the high powder content. The hardness is in the range 550 HV and 750 HV in the dendritic structure. However, the hardness in the scope of 890 HV and 1210 HV were estimated in the hypereutectic structures. The lower hardness of

dendritic microstructure was related to commonly a low groupings of Fe, Cr, Si, C and nearness of fundamental dendrites.

Saravanan R et al. [13] The primary point of this undertaking is to alter the outside of LM 25 ingot so as to have a refined microstructure, improvement in hardness and in the wear rate of the adjusted area. Techniques: Surface change of LM 25 is done utilizing GTA strategy. Argon stream was limited and all the while unadulterated nitrogen (99.999%) was brought into the earth. Microstructural perception was done utilizing Zeiss Axiovert 25CA metallurgical magnifying instrument and the hardness was estimated utilizing Mitutoyo Vicker's hardness trying machine. Wear test was done for the substrate and the altered district utilizing pin-on-plate wear analyzer. EDAX examination was done to discover the nearness of intermetallic mixes. From the microstructure, it was seen that there is grain refinement in the adjusted area. The hardness for the substrate was observed to be 80.6 HV and 764.4 HV for the changed district. The wear rate in the substrate was 49.34x10⁻⁴ mm³/m and 7.9x10⁻⁴ mm³/m for the adjusted area. As the hardness builds, wear rate diminishes. EDAX report affirms the nearness of intermetallic compound as silicon nitride (Si₃N₄). The nearness of the silicon nitride isn't accounted for already utilizing GTA as warmth source on surface changed LM25. The expansion in the hardness and lessening in the wear rate is ascribed to the nearness of silicon nitride in the surface. Because of the nearness of silicon nitride it very well may be utilized as a protector and synthetic boundary in electrical circuits and so forth. It can likewise have more extensive car and air transportation applications as its hardness has expanded.

Vijay Narayanan et al.[14]Stainless steels are for the most part utilized where aversion of erosion assault is the fundamental criteria, however low surface hardness and high wear rate are key hindrances to broad application. Techniques: The surface alloying of AISI 304 tempered steel with titanium was done utilizing the warmth created from the Gas Tungsten Arc (GTA). Analyses were directed by fluctuating the GTA parameters and the ideal parameter was resolved. Organization of the surface alloyed layer was broke down utilizing nuclear outflow spectrometer. The Ti alloyed surface layers were portrayed utilizing SEM imaging/EDAX investigation. Piece of the surface alloyed layer was dissected utilizing nuclear emanation spectrometer and the outcomes affirmed an expansion in the Ti content superficially layer when contrasted with the synthesis of the substrate. The EDAX examination demonstrated that intermetallic

compounds are available in the Ti alloyed surface layers. The microhardness was estimated utilizing the Vickers microhardness testing machine and the hardness expanded from 267.5 HV for the substrate to 2098 HV for the surface alloyed layer. The wear was estimated utilizing the stick on-plate wear analyzer and the wear rate diminished from 14.78×10^{-4} mm³/m for the substrate to 1.84×10^{-4} mm³/m for the surface alloyed layer. The perception of the microstructure uncovered that there is grain refinement in the Ti alloyed surface layer. The altered examples can be utilized as medicinal inserts, control poles in atomic power plants, siphon barrels petrochemical industry. This technique can be utilized to improve the properties in explicit territory of an item.

III. EXPERIMENTAL PROCEDURE

3.1 Introduction

This chapter discusses the materials and methods used in this research. The chapter presents details on the experimental work carried out including the experimental set up, experimental matrices and various testing methods used for the present investigation. The experimental setup and procedures are explained as follows.

3.2 Experimental Setup

The equipment's used in the present study are;

- a) Bios D.C Invertor Gas Tungsten Arc (GTA) equipment as the heat source for surface Alloying Process at DCEN mode.
- b) Linear manipulator driven by a servo motor with a PLC controller incorporated in GTA equipment for the substrate movement.
- c) Zeiss Metallurgical Microscope for microstructural examination.
- d) Mitutoyo micro- hardness tester for hardness measurement.
- e) DUCOM pin-on-disc wear testing machine with LVDT sensors and data acquisition software for wear and friction tests.
- f) Zeiss Zigma Field Emission Scanning Electron Microscope for SEM/EDAX (Energy Dispersive X-ray Spectrometry)

3.3 General Procedure

3.3.1 Specimen Preparation

The AISI304 stainless steel substrate is machined into the dimension of 30x30x150 mm and the surface is polished using emery paper. The surface is then cleaned with acetone to remove dirt, grease, oil etc. Ti sheet of 300 μm and Copper sheets of 0.7 and 1 mm thick were cut into 30x150 mm rectangular sheets and cleaned with acetone.

3.3.2 Surface Alloying Process

The machined specimen (Substrate) was mounted on the working table. On top of the substrate, the cut CP-Ti and Cu sheets were placed. The GTA torch was held stationary for all the set of experiments. The specimen mounted on the working table was set to move with a specified speed as per the requirement using the linear manipulator [15]. Thoriated (2.2%) Tungsten electrode of diameter 2.4 mm was used. The specimen was placed such that the electrode lies above the specimen at its one end. Nitrogen (N₂) gas of ultrahigh purity was used as the shielding gas with a flow rate of 12 litre/min. The GTA torch moves across on the top surface of the specimen melting both the Ti and Cu onto the top surface of the substrate thereby causing surface alloying process to occur. The GTA equipment is shown in Figure 3.1.

3.3.3 Design of Experiments (DOE)

3.3.3.1 Identification of Parameters

From pervious literature, factors which shows the maximum influence on the weld bead geometry in the Gas Tungsten Arc (GTA) welding have been recognized and the following factors that are considered in this study are namely welding current (Amps), welding speed (mm/sec) and stand-off distance (mm).

3.3.3.2 Finding the working limits of the parameters

Various trail runs were performed on SS-Ti to discover the powerful and achievable working points of confinement of the Gas Tungsten Arc (GTA) welding parameters incorporated into this investigation according to the condition appeared Table.

Table 3.1 Welding Conditions

Polarity	DCEP (Electrode Positive)
Electrode	2% thoriated tungsten electrode
Electrode Diameters	2.4 mm
Shielding Gas	Nitrogen (N ₂)
Gas Flow Rate	12L/min
Torch Position	180° Flat
Operation	Semi-Automatic

Table 3.2 Process parameters and their values at various levels

S.No	Factors	Units	Levels		
			-1	0	1
1	Current	Amps	160	180	200
2	Travel Speed	mm/sec	1	2	3
3	Stand-off Distance	mm	2	3	4

- With current less than 160 Amps, the Ti sheet got melted and not fused with the substrate.
- If travel speed exceeds 3 mm/sec, fusion zone does not occur.
- For stand-off distance higher than 4 mm, substrate does not melt and in below 2 mm, the liquid metal splashes out.

3.3.3.3 Developing Experimental Data

Based on the above observations, range of the working parameters has been considered: for current (160-180 Amps), travel speed (1-3 mm/sec) and stand-off distance (2-4 mm) i.e., the welding has been performed without any defects. The effects of process parameters onto the output response was studied using a 3-parameters and 3-level Central Composite Design (CCD) in the form of Response Surface Methodology (RSM). Table shows the considered process parameters and its levels and Table shows the DOE table with responses.

Table 3.3 3-factor CCD matrix and Response value

Ex. No	Current (Amps)	Speed (mm/sec)	Distance (mm)
1	160	3	2
2	180	2	3
3	180	1	3
4	200	3	4
5	160	1	4
6	180	3	3
7	180	2	3
8	200	3	2
9	180	2	3
10	200	1	2

11	160	1	2
12	180	2	3
13	180	2	4
14	180	2	2
15	180	2	3
16	160	2	3
17	200	1	4
18	200	2	3
19	160	3	4
20	180	2	3

3.4 Experimental Phase in the Present Study

In this phase Surface Alloying Process was carried out on the AISI304 Stainless steel with Ti by varying the GTA process variables. The optimal process parameter was identified and further specimens are prepared using it. Microstructural examination, hardness measurement of the substrate and the surface alloyed specimens were studied.

3.4.1 Procedure

AISI304 stainless steel specimens were procured in wrought form. The chemical composition of the alloy specimens was analyzed using arc spectrometry. The chemical composition was found to be within the range of ±0.2wt% of the nominal composition. The chemical composition of the alloy used is reported in Table 3.4. The AISI304 stainless steel specimens were machined into square bars of dimension 150 x 30 x 30 mm. The machined AISI304 stainless steel substrate is shown in Figure 3.2.



Figure 3.1 Machined specimen of AISI304 Stainless steel specimen

Figure 3.3 shows the commercially pure titanium sheet of 0.3 mm and the copper sheet of 0.7 and 1 mm thickness.



Figure 3.2 Ti of 0.3 mm thick sheet

Surface Alloying Process was carried out on the AISI304 stainless steel substrate with Ti and Cu using GTA heat source. In the phase 1, the experiments were repeated with varying GTA process variables.

The optimal parameter was identified based on the hardness obtained in each process parameter set used. A 2.2% thoriated tungsten electrode was used for the surface alloying process. The fixed parameters are electrode diameter – 2.4mm, Nitrogen (N₂) – 12 L/min. The surface alloyed specimens were cut using wire cutting method to prepare specimens for microstructural observation.

3.5 Testing Methods

Microstructural examination and the surface hardness testing were carried out for the substrate and the surface modified specimens. The testing procedures are explained as follows:

3.5.1 Microstructural Examination

Microstructure of substrate and refined specimens were examined using an optical metallurgical microscope (Make: Zeiss; Model: 25CA) as shown in Figure 3.3. The specimens were prepared using standard metallographic techniques and etched with Waterless Kaling's reagent [16].

The optical metallurgical microscope which is capable of reproducing the microscopic images at a magnification factor ranging from 100X to 500X was used. The images were captured and recorded using a CCD camera with an image processing software (Motic Images plus 2.0).



Figure 3.3 Zeiss metallurgical microscope

3.5.2 Hardness Testing

To evaluate the effect of Surface Modification Process, the hardness of the substrate and the modified alloy specimens were measured using micro-hardness tester (Make: Mitutoyo; Model: MVK – H11)[17]. Several readings were taken at the top surface and different locations along the depth of the modified layer for each specimen and an average value was calculated. The specimens were prepared and tested as per ASTM E384 standard. The parameters used in this test were: 100 gm.-f applied load for a duration of 15 s. The hardness values varied in each sample was within ± 10 HV. The Vicker's hardness tester is shown in Figure 3.4.



Figure 3.4 Vicker's hardness tester

3.5.3 Wear Testing

(a) Height loss versus time (b) Coefficient of friction versus time and (c) Frictional force versus time. ASTM G99 standard test method was used to conduct the test. The experimental setup is shown in the Figure3.5.



Figure 3.5 pin-on-disc wear tester

Table 3.5 Wear and friction testing parameters

S.No	Test	Unit	Value
1	Rotational Speed	rpm	424
2	Velocity	m/s	2.5
3	Track diameter	mm	110
4	Sliding Time	s	600
5	Sliding distance	m	1500
6	Load applied	N	20

3.5.5 XRD analysis

The intermetallic compound formation in the substrate and the surface alloyed layer were confirmed using XRD analysis. The XRD equipment used for the testing purpose is PAN Analytical X-pert pro Shown in Figure 3.7.



Figure 3.7 PANalytical X'Pert Pro XRD machine

3.6 Conclusion

The following experimental details and methods were explained in this chapter:

- a) Sample preparation for Surface Alloying Process.
- b) The detailed experimental procedure.
- c) The property evaluation techniques like microscopic examination, micro-hardness test, wear test, SEM/EDAX analysis and XRD analysis.

IV. EFFECT OF Ti SURFACE ALLOYING PROCESS ON THE MICROSTRUCTURE, THE HARDNESS AND THE WEAR RATE OF AISI304 STAINLESS STEEL

4.1 Introduction

This chapter discusses an investigation on the effect of the surface alloying process on the microstructure and the surface hardness of the surface alloyed AISI304 stainless steel since a study using GTA as the heat source under nitrogen environment has not been reported previously.

The substrate was machined to the required size of 100 x 30 x 30 mm. CP-Ti sheets of 300µm were used as the source for the Ti addition. Surface alloying process was carried out on the substrate using GTA heat source to melt the substrate surface and the Ti sheet so as to form a surface alloyed layer on solidification. Arc spectrometry was used to measure the composition of the surface alloyed specimen.

The surface alloyed specimens were prepared for microstructural observation using the conventional metallurgical techniques. Hardness measurements were carried out on the cross section of the surface alloyed layer. Further SEM/EDS analysis were carried out to study the phase formations on the surface alloyed layer[18]. XRD analysis were performed in order to confirm the compounds formed during the surface alloying process of AISI304 stainless steel with Ti.

4.2 Results and Discussion

The surface alloyed AISI304 stainless steel specimen with the surface alloyed layer formed on the top surface of the substrate after Surface alloying with 300 µm thick Ti sheet was shown in Figure 4.1.



Figure 4.1 Ti surface alloyed AISI304 Stainless steel specimen

4.2.1 Depth of Penetration

Fig. 4.2a-c shows the effect of heat input on the cross sections of the Ti modified specimens. It is observed that the depth of penetration varies with heat input, which is derived from the equations (2 & 3).

- Arc Energy = (Voltage × Current) / Travel speed (Equation 2)
- Heat Input (HI) = 0.8 × Arc Energy (KJ/mm) (Equation 3)

It is understood that the process parameters like current and travel speed plays an important role in deciding the penetration by heat input. Each arc characteristics has a value denoting its process efficiency which is for example 0.8 in GTAW. HI is the energy consumed in forming unit length of modified surface. But it is more significant if the HI have high/low value due to several reasons since it controls cooling rate thereby controlling the grain size. The depth was clearly observed with the constant voltage value of 15KV and the variation in process parameters of current and travel speed (160 Amps, 3 mm/sec), (180 Amps, 2 mm/sec) and (200 Amps, 1 mm/sec) were shown in fig. 1a-c.

Depth of Penetration	Heat Input
	640 KJ/mm
	1080 KJ/mm
	2400 KJ/mm

Figure 4.2a-c Effect of Heat input on the cross section of Ti modified specimens

4.2.2 Microstructure Analysis

Microstructure of the AISI304 SS substrate was shown in Figure 4.3 (a). The black stringers show the presence of carbides and delta ferrite scattered in the austenitic matrix and steps between grains and annealing twin boundaries are shown in top right-hand corner.

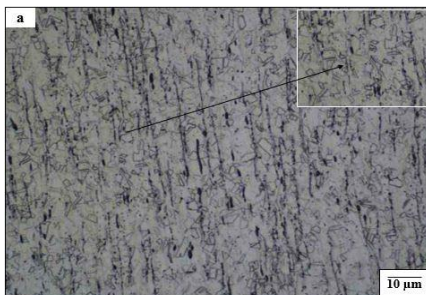


Figure 4.3 a Microstructure of AISI304 stainless steel substrate

Figure 4 (b) shows the microstructure of the Ti modified SS with process parameters (180 Amps, 2

mm/sec and 3 mm). A very finely refined grain structure were observed due to the addition of Ti which act as a grain refiner and the black spots shows the presence of rich iron phase. The formation of TiN is evident with a gold colour scattered (top left-hand corner) in the matrix [16].

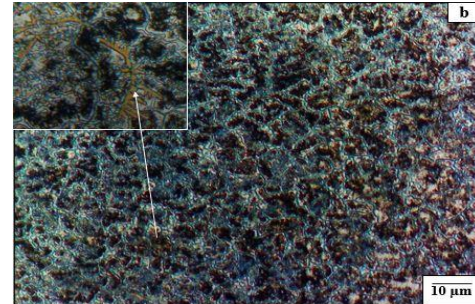


Figure 4.3 b Microstructure of Ti modified layer

Microstructure of the Ti modified SS with process parameters (200 Amps, 1 mm/sec and 2 mm) was shown in Figure 4 (c). The dendritic structure were observed in the matrix. The diffusion of Ti and nitride were very less because due to the increase in welding current and decrease in travel speed and distance, the higher amount of heat transfer possess low diffusion rate of titanium and the time for solidification of weld pool becomes longer, so the nitrogen may be released from the molten pool.

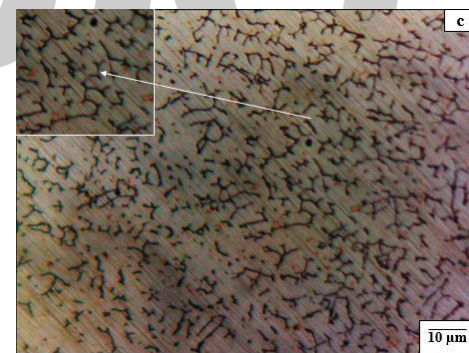


Figure 4.3 c Microstructure of the Ti modified layer

4.2.3 Phase Identification

The formation of the intermediate compounds in the surface alloyed layer was identified and confirmed using SEM imaging, EDS and XRD analysis.

4.2.3.1 SEM imaging

Figure 4.4 presents SEM micrograph of the cross section of the Ti modified layer. According to these figures, the amount of TiN (dark spots) were observed using scanning electron microscope. The eutectic structure in the sample, which appears like grain boundary segregation, are shown at higher magnification in the left-hand corner. The TiN phase is

an extremely hard intermediate compound usually on the order of 2500-3000 HV, which is one of the reasons behind the drastic increase in hardness of the AISI304 SS substrate.

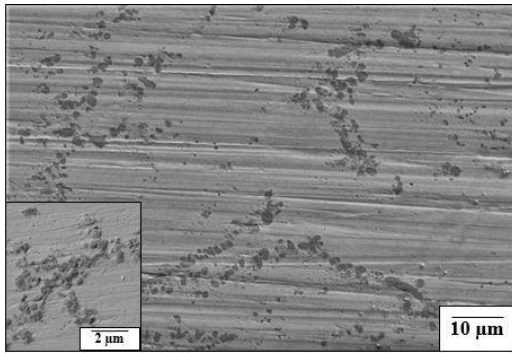


Figure 4.4 Presence of TiN using SEM imaging

4.2.3.2 EDS analysis

Energy Dispersive Spectroscopy (EDS) spectrum for Ti modified layer on SS304 is shown in Figure 4.5 and 4.6. The analysis were conducted at the center point on the cross section of the modified region and it shows the presence of different titanium-nitride and nickel-titanium composition. 51.57 wt. % Ti with 48.43 wt. % N and 60.72 wt. % Ni with 39.28 wt. % Ti was observed in the modified layer. The formation of intermediate compounds was observed in Figure 4.5 and Figure 4.6.

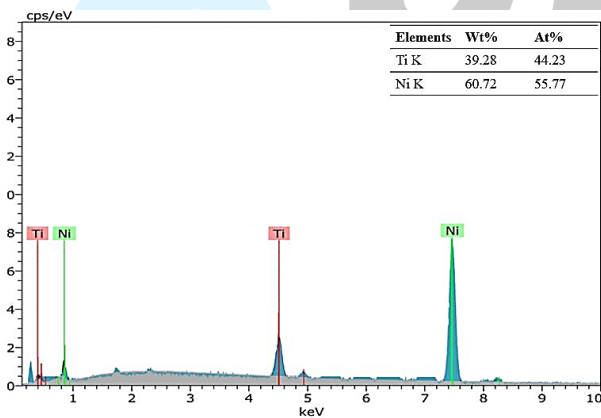


Figure 4.5 EDS plots for TiNi

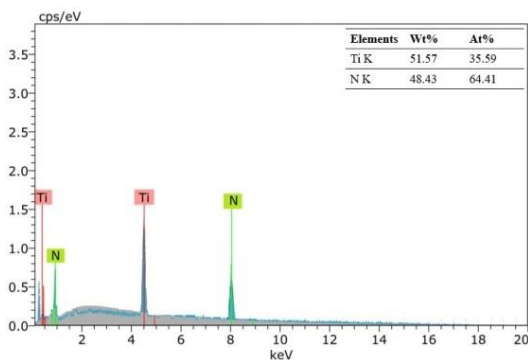


Figure 4.6 EDS plots for TiN

4.2.3.3 XRD analysis

X-Ray Diffraction (XRD) analysis were performed to predict the phase present in the Ti modified region using PAN Analytics equipment. From figure 4, the spectra has sharp peaks indicating good crystallinity but show distinct features which gives indications of the compositions in the modified region. The peaks with angles 42.6°, 43.86°, 44.68°, 64.74° and 81.98° corresponds to TiN (AMCSD: 0017997), FeNi (JCPDS: 65-7753) and TiNi (AMCSD: 0018897) phases.

It is to be noted that the surface modification carried out in this study is a non-equilibrium process with very fast heating and ambient cooling. Intermediate compounds of different compositions could get precipitated during the heating/cooling process that do not have enough time to homogenize through diffusion. Thus, it may be concluded that surface modification of the substrate with Ti under N₂ shielding gas results in the formation of very finely refined grain structures and titanium nitride particles distributed in the matrix.

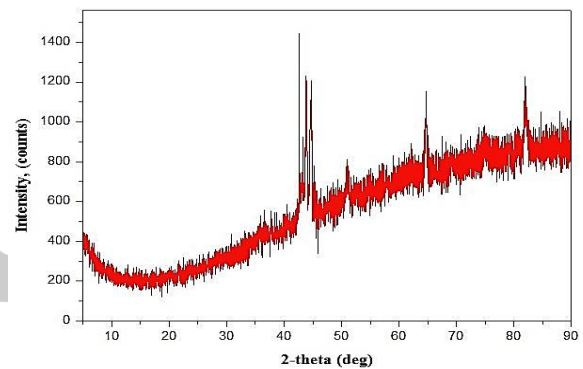


Fig. 4.7 Hardness value of Ti modified layer along depth direction with process parameters

4.2.4 Hardness Profiles

Fig. 4.7 shows the hardness value of Ti modified layer along depth direction with process parameters (Current 180 Amps, Travel Speed 2 mm/sec, Stand-off Distance 3 mm) i.e. Ex. 15. The hardness value measured on the cross sections of the substrate is 264HV and for Ti modified layer the average hardness was measured to be 2679HV.

The significant increase in hardness is due to the formation of intermediate phases like TiN, FeNi and TiNi at the modified layer. The improvement of hardness is directly related to N₂ dissolution in the melt zone.

This high N₂ concentration in the Ti modified region resulted in the formation of TiN population and refined dendrites during solidification, which ultimately caused the hardness to increase. The hardness value varies

along the depth direction due to the difference in the cooling rate or solidification after SA. The rate of diffusion of titanium is more in the top surface and the Ti diffusion in the modified layer decrease towards the depth direction [19].

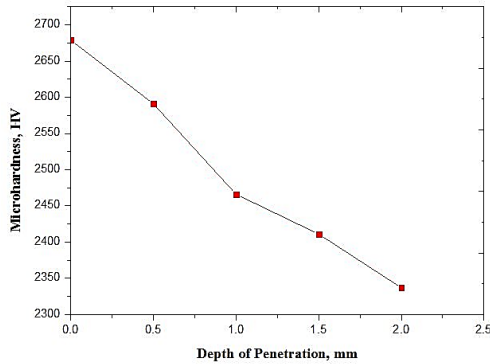


Figure 4.7 Hardness vs Depth from Top Surface

4.2.5 Comparison of Hardness Data

Figure 4.8 bar chart shows that the hardness values obtained in this study for the Ti surface alloyed AISI304 SS under N₂ environment is significantly higher than that of the value for the substrate. This observation is consistent with that of the previous studies using laser and GTA as the heat source. Further, the results of this study is comparable to those of Anandan et al. (2012), Buytoz & Ulutan (2006), Mridha (2005) and Vijay Narayanan et al. (2016). All researchers compared were conducting using AISI304 SS as the substrate. The variation is due to the improvement in the surface hardness of AISI304 SS with Ti modified region is due to the presence of the hard intermediate phases TiN, FeNi and NiTi with a refined dendrite structure.

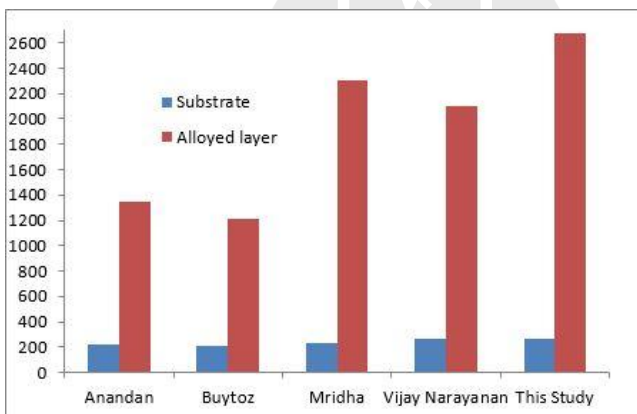


Figure 4.8 Hardness data comparison of different surface alloying process with this study

4.2.6 Wear Rate

Wear testing was done on the substrate and the Ti modified specimens using Pin-on-Disc wear tester with a diamond like coating disc. The wear was calculated

in terms of weight loss which was derived from the equation (1).

- Wear in terms of weight loss = $\Delta m / \rho \times l$ mm³/m (Equation 1)
- Where, Δm = Original volume – change in volume (g)
- ρ = density of AISI304 SS and titanium (g/mm³)
- l = sliding distance (m)

The wear rate of AISI304 SS substrate and the Ti modified specimens. The value of the wear rate were reduced from 0.430×10^{-3} mm³/m for the substrate to 0.0015×10^{-3} mm³/m and 0.220×10^{-3} mm³/m for the Ti modified layer of process parameters (Current 180 Amps, Travel Speed 2 mm/sec, Stand-off Distance 3 mm and Current 200 Amps, Travel Speed 1 mm/sec, Stand-off Distance 2 mm). The decrease in wear rate is due to the formation of intermetallic phases TiN, FeNi and TiNi in the Ti modified specimens. The variation in wear rate value were observed for Ti modified specimens (i.e., Ex 15 and Ex 10) because the existence of TiN are different. Because when the welding current increases, the solidification time becomes longer and release of nitride content from the molten pool get increased.

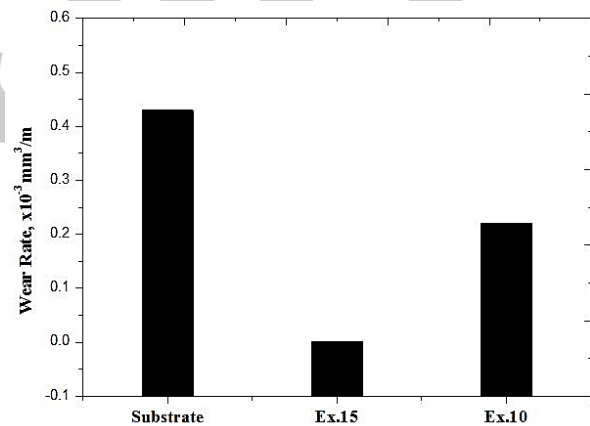


Figure 4.9 Comparison of wear rate for substrate and Ti modified specimens

4.3 Conclusion

Based on the results of this investigation, the following conclusions are drawn:

1. The SA process of AISI304 SS with Ti under nitrogen environment enhances the microstructure due to fast cooling occurring in the process.
2. The surface hardness values of the substrate was measured to be 264HV and for surface alloyed layer of Ti were measured to be 2679HV.
3. The increase in hardness is credited to the formation of intermediate phases TiNi, FeNi and

TiN with refined grains and dendrites structure due to the variation in the cooling rate.

4. The hardness shows a gradient in the depth direction within the Ti alloyed layer due to the difference in the cooling rate.
5. It is observed that the value of wear rate decreases from $0.430 \times 10^{-3} \text{ mm}^3/\text{m}$ for the substrate to $0.0015 \times 10^{-3} \text{ mm}^3/\text{m}$ and $0.220 \times 10^{-3} \text{ mm}^3/\text{m}$ for the Ti modified layer of process parameters (Current 180 Amps, Travel Speed 2 mm/sec, Stand-off Distance 3 mm and Current 200 Amps, Travel Speed 1 mm/sec, Stand-off Distance 2 mm).
6. It is observed that the process parameters have significant effect on the surface hardness and wear rate while it affects the width and depth of the Ti SA layer.
7. The GTA heat source can be considered as an alternate heat source to laser/e-beam for the SA of AISI304 SS.

V. OPTIMIZATION OF GTA PROCESS PARAMETERS

5.1 Introduction

This chapter discusses an optimization of GTA process parameters on the AISI304 SS with Ti under N₂ environment since a DOE analysis using GTA under nitrogen as shielding gas has not been reported previously.

In this study design expert's 10.0.6 software has been used to perform the optimization through response surface methodology. Process parameters and output response is given in Table 5.1.

5.2 Depth of Penetration

Analysis of variance results for the response surface model of depth is given in Table 6. The F-value 47.15 indicates that the model is significant.

There is only 0.01% chance that large value of F could occur due to noise. Values of "Prob> F" less than 0.0500 indicates the model terms are significant.

In this case A, B, BC and A² are significant model terms. Values that are (> 0.1) such as C, AB, AC, B², C² terms are not significant.

If there are many insignificant model terms, model reduction were used to improve the model.

$$SD= 0.20, \text{ Mean}= 3.09, R^2= 0.9263, \text{ Adj } R^2= 0.9067$$

The "R-Squared" value of 0.9263 is in sensible agreement with the "Adj R-Squared" value of 0.9067;

i.e. the difference is less than 0.02. Equation (4) shows the regression analysis for depth of penetration.

Figure 9 shows the 3D surface profile for the response depth of penetration with a current of 180 Amps.

$$\text{Depth of penetration} = +28.96000 - (0.29950 \times \text{Current}) - (0.65000 \times \text{Speed}) - (3.91921\text{E-}016 \times \text{Speed} \times \text{Distance}) + (9.00\text{E-}004 \times (\text{Current}^2)) \dots \dots (\text{Equation 4})$$

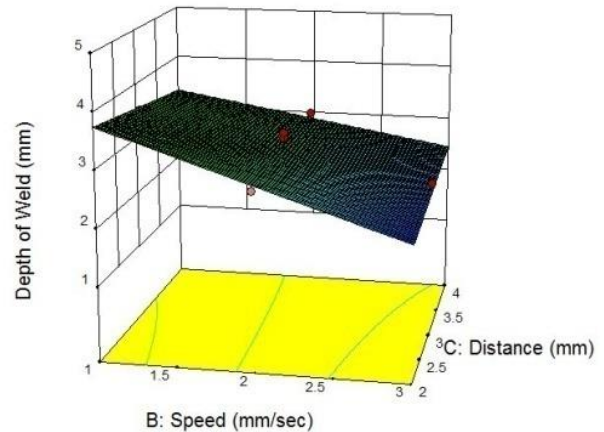


Figure 5.1 3D surface plot for depth of penetration

5.3 Hardness Value

Table 7 shows the analysis of variance results for the response surface model of hardness value. The F-value 8.80 denotes that the model is significant. There is only 0.07% of chance that a large value of F could arise due to noise.

Values of "Prob> F" is less than 0.5000 indicates that the model are significant. In this case A, BC, B² are significant model terms.

The remaining model terms such as C, AB, AC, A², C² are not significant (i.e. values greater than 0.1). Model reduction were used to remove the insignificant terms in order to develop the model.

$$SD= 300.08, \text{ Mean}= 1999.80, R^2= 0.7013, \text{ Adj } R^2= 0.6216$$

There is a reasonable agreement with "R-Squared and Adj R-Squared" values of 0.7013 and 0.6216 i.e. the difference is less than 0.08. Equation (5) developed the regression analysis for hardness value.

Figure 10 shows the 3D surface plots for the hardness value with a value of current as 180 Amps.

$$\text{Hardness} = +1366.80000 - (10.67000 * \text{Current}) + (2907.55000 * \text{Speed}) - (60.58333 \times \text{Speed} \times \text{Distance}) - (644.00000 \times (\text{Speed}^2)) \dots \dots (\text{Equation 5})$$

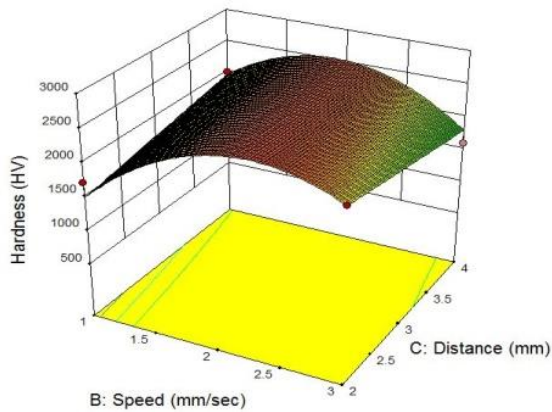


Figure 5.2 3D surface plot for Hardness

5.4 Wear Rate Value

Analysis of variance for the response surface model for wear rate value are presented in Table 8. The F-value 9.54 indicates that the model is significant. There is only 0.05% chance of occurring large value of F due to noise.

Values of “Prob> F” less than 0.5000 implies that model terms are significant. In this case A, B, BC, B² are significant model terms. Values such as C, AB, AC, A², C² terms are greater than 0.1 are not significant. Using model reduction, the non-significant model terms are eliminated to have a better improved model.

$$SD = 0.034, \text{ Mean} = 0.043, R^2 = 0.7328, \text{ Adj } R^2 = 0.6616$$

It is understood that the “R-Squared” value of 0.7328 is in sensible agreement with the “Adj R-Squared” value of 0.6616 (i.e. the difference is less than 0.07). Equation (6) shows the regression analysis for wear rate. Figure 11 shows the 3D surface profile for wear with a current of 180 Amps.

$$\text{Wear Rate} = +5.82000\text{E-}003 + (1.71500\text{E-}003 \times \text{Current}) - (0.27826 \times \text{Speed}) + (3.66667\text{E-}003 \times \text{Speed} \times \text{Distance}) + (0.058540 \times (\text{Speed}^2)) \dots \dots \dots (\text{Equation 6})$$

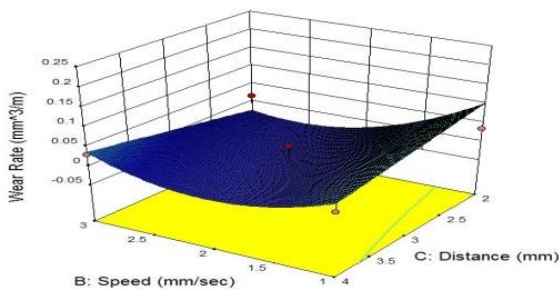


Figure 11 3D surface plot for Wear Rate

5.5 Model Validation

The optimized process parameters have been verified by conducting different validations. For validating,

new set of process parameters were considered for surface modification. The experiment run was performed and the depth of penetration, the hardness and the wear rate is measured and compared with the values of each response calculated from the equations (1-3) were given in the Tables (9-11).

VI. CONCLUSION AND SCOPE OF FUTURE WORK

The following conclusions are drawn based on the results obtained after Surface Alloying Process of AISI304 stainless steel with Titanium.

6.1 Conclusion based on effect of Ti surface alloying process on the Microstructure, the Hardness and the Wear Rate of AISI304 Stainless Steel

1. The SA process of AISI304 SS with Ti under nitrogen environment enhances the microstructure due to fast cooling occurring in the process.
2. The surface hardness values of the substrate were measured to be 264HV and for surface alloyed layer of Ti were measured to be 2679HV.
3. The increase in hardness is credited to the formation of intermediate phases TiNi, FeNi and TiN with refined grains and dendrites structure due to the variation in the cooling rate.
4. The hardness shows a gradient in the depth direction within the Ti alloyed layer due to the difference in the cooling rate.
5. It is observed that the value of wear rate decreases from $0.430 \times 10^{-3} \text{ mm}^3/\text{m}$ for the substrate to $0.0015 \times 10^{-3} \text{ mm}^3/\text{m}$ and $0.220 \times 10^{-3} \text{ mm}^3/\text{m}$ for the Ti modified layer of process parameters (Current 180 Amps, Travel Speed 2 mm/sec, Stand-off Distance 3 mm and Current 200 Amps, Travel Speed 1 mm/sec, Stand-off Distance 2 mm).
6. It is observed that the process parameters have significant effect on the surface hardness and wear rate while it affects the width and depth of the Ti SA layer.
7. The GTA heat source can be considered as an alternate heat source to laser/e-beam for the SA of AISI304 SS.

6.2 Conclusion based on optimization of GTA process parameters: Scope for future work

1. Corrosion studies at elevated temperature and different solution medium can be carried out on the Ti Surface Alloyed AISI304 stainless steel specimen.

2. The effect of oxidation on the hardness and wear rate of Ti surface alloyed AISI304 stainless steel can be carried out.
3. The Wear behavior of the surface alloyed specimens can be studied by changing the wear testing parameters including temperature.

REFERENCES

- [1] Handbook, W., "Welding processes", American Welding Society, Vol. 2, (1991), 8-14.
- [2] Kalpakjian, S. and Schmid, S.R., "Manufacturing engineering and technology, Pearson Upper Saddle River, NJ, USA, (2014).
- [3] Jiménez-Come, M., Turias, I. and Trujillo, F., "An automatic pitting corrosion detection approach for 316L stainless steel", Materials & Design, Vol. 56, (2014), 642-648.
- [4] Lo, K.H., Shek, C.H. and Lai, J., "Recent developments in stainless steels", Materials Science and Engineering: R: Reports, Vol. 65, No. 4, (2009), 39-104.
- [5] Handbook, W., "AWS", Welding Processes, Vol. 2, (1991).
- [6] Shanping, L., Hidetoshi, F. and Kiyoshi, N., "Effects of CO₂ shielding gas additions and welding speed on gta weld shape", Journal of Materials Science, Vol. 40, No. 9-10, (2005), 2481-2485.
- [7] Liao, M. and Chen, W., "The effect of shielding-gas compositions on the microstructure and mechanical properties of stainless steel weldments", Materials Chemistry and Physics, Vol. 55, No. 2, (1998), 145-151. 8. Kou, S., "Welding metallurgy, John Wiley & Sons, (2003).
- [8] Hebda, M. and Sady, R., "Software for the estimation of steel weldability", Advances in Engineering Software, Vol. 58, (2013), 13-17.
- [9] Choudhary, S. and Duhan, R., "Effect of activated flux on properties of ss 304 using tig welding", International Journal of Engineering-Transactions B: Applications, Vol. 28, No. 2, (2014), 290-298.
- [10] Doniavi, A., Hosseini, A. and Ranjbary, G., "Prediction and optimization of mechanical properties of st52 in gas metal arc weld using response surface methodology and anova", International Journal of Engineering-Transactions C: Aspects, Vol. 29, No. 9, (2016), 1307-1313.
- [11] Zarooni, M. and Eslami-farsani, R., "Effect of welding heat input on the intermetallic compound layer and mechanical properties in arc welding-brazing dissimilar joining of aluminum alloy to galvanized steel", International Journal of Engineering-Transactions B: Applications, Vol. 29, No. 5, (2016), 669-678.
- [12] Sathiya, P., Mishra, M.K. and Shanmugarajan, B., "Effect of shielding gases on microstructure and mechanical properties of super austenitic stainless steel by hybrid welding", Materials & Design, Vol. 33, (2012), 203-212.
- [13] Palani, P. and Murugan, N., "Modeling and simulation of wire feed rate for steady current and pulsed current gas metal arc welding using 317L flux cored wire", The International Journal of Advanced Manufacturing Technology, Vol. 34, No. 11, (2007), 1111-1119.
- [14] Kumar, S. and Shahi, A., "Effect of heat input on the microstructure and mechanical properties of gas tungsten arc welded aisi 304 stainless steel joints", Materials & Design, Vol. 32, No. 6, (2011), 3617-3623.
- [15] Gülenç, B., Develi, K., Kahraman, N. and Durgutlu, A., "Experimental study of the effect of hydrogen in argon as a shielding gas in mig welding of austenitic stainless steel", International Journal of Hydrogen Energy, Vol. 30, No. 13, (2005), 1475-1481.
- [16] RajaKumar, G., Ram, G. and Rao, S., "Microstructure and mechanical properties of borated stainless steel (304b) gta and sma welds", La MetallurgiaItaliana, No. 5, (2015).
- [17] Kurt, H.I. and Samur, R., "Study on microstructure, tensile test and hardness 304 stainless steel jointed by tig welding", International Journal of Science and Technology, Vol. 2, No. 2, (2013), 163-168.
- [18] Standard, A., "A370-12a", Standard Test Methods and Definitions for Mechanical Testing of Steel Products, (2012).